DIRECT MEAN TORQUE CONTROL OF AN INDUCTION MOTOR

E. Flach, R. Hoffmann, P. Mutschler

Institute for Power Electronics and Electrical Drives
Darmstadt University of Technology, Germany

Abstract: A new method to control flux and torque of an induction motor is presented. Direct Mean Torque Control (DMTC) combines the good dynamic performance of Direct Torque Control (DTC) with the advantages of time equidistant control algorithms for digital implementation in signal processor based systems. Experimental results confirm the validity of the control scheme.

Keywords: Direct Torque Control, Induction Machine, Digital Control, Constant Cycle Time

INTRODUCTION

Classical field orientation has achieved a good performance in many applications where a converter with high switching frequency is used. In this case, a microcontroller may satisfy the needs of calculation power.

Direct methods achieve a higher dynamic performance since they do not use a modulator, i. e. a PWM. Using comparators with hysteresis, analog devices are commonly used to realise Direct Torque Control (Takahashi and Noguchi [1]) or similar methods. An entirely digital implementation seems to be interesting to avoid additional analog components, but it is a computation intensive task to control every switching event, particularly when a sophisticated model of the machine is required. Induction motors with small leakage inductance leading to fast current change promise excellent dynamics, but require short pulse intervals to decrease torque ripple. The computational expenditure necessary to realise short pulse intervals seems to be too expensive for an entirely digital implementation, and maybe slightly exaggerated too. On the other hand, the switching interval varies in a wide range. At high and low speed, long and short switching intervals alternate. If one has to keep the torque in a preset hysteresis-band with a minimum of switching events, Depenbrock [2] is best suited, but current harmonics are rather large. Reduced current harmonics but some more switching events are generated by [1].

If current harmonics are to be reduced, constant switching frequency is preferable. Additionally, digital implementation calls for constant switching frequency.

CONTROL STRATEGY

Basic Control Scheme

Fig. 1 shows the control structure of DMTC. It uses constant switching frequency and determines the switching events in advance for a fixed cycle Δt_{cycle}.

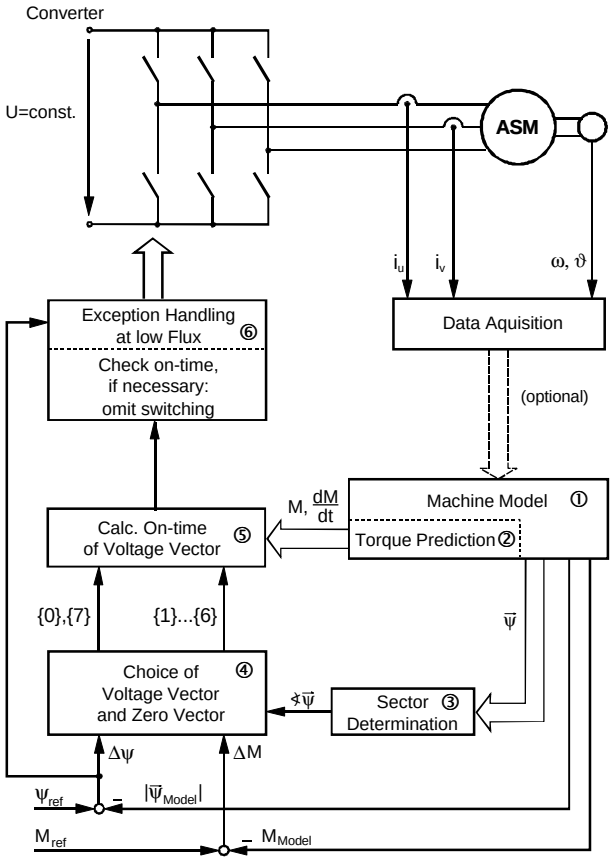

Figure 1: Control structure of DMTC

The switching events are directly scheduled in a way that the mean torque over the cycle is equal to the

desired value. In most cases, switching a voltage vector (VV) and a zero voltage vector (ZV) satisfies the demand. In general, there are always two VVs to influence the torque in the desired manner. The choice of the adequate VV is made by the flux controller in a way that the flux deviation at the end of the on-time of the VV is minimal.

Torque[1)] Control

Fig. 2 shows a typical cycle of operation, which may be similar to those of the control scheme proposed in [1] in steady state. Applying a voltage vector first, the torque increases at the beginning. Then, applying a zero vector, the torque decreases. The object is to equalise the differently hatched areas.

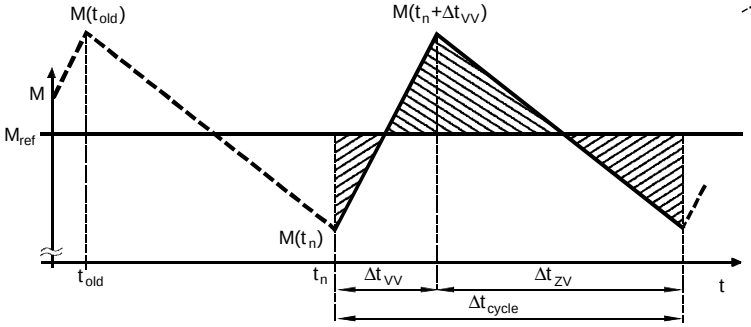

Figure 2: Typical cycle of operation of DMTC

The motor can be modelled in a stator reference (a, b) by the following equation:

$$\frac{d}{dt}\begin{bmatrix}\psi_{sa}\\ \psi_{sb}\\ \psi_{ra}\\ \psi_{rb}\end{bmatrix}=\begin{bmatrix}-\frac{R_s}{\sigma L_s} & 0 & \frac{R_s L_h}{\sigma L_s L_r} & 0\\ 0 & -\frac{R_s}{\sigma L_s} & 0 & \frac{R_s L_h}{\sigma L_s L_r}\\ \frac{R_r L_h}{\sigma L_s L_r} & 0 & -\frac{R_r}{\sigma L_r} & -n_p\cdot\omega_m\\ 0 & \frac{R_r L_h}{\sigma L_s L_r} & n_p\cdot\omega_m & -\frac{R_r}{\sigma L_r}\end{bmatrix}\cdot\begin{bmatrix}\psi_{sa}\\ \psi_{sb}\\ \psi_{ra}\\ \psi_{rb}\end{bmatrix}+\begin{bmatrix}u_a\\ u_b\\ 0\\ 0\end{bmatrix} \quad (1)$$

Eq. (1) is solved online in the block "Machine Model" of Fig. 1 using Runge-Kutta integration of second order. For this model, the torque is given by

$$M = n_p \frac{L_h}{(L_s L_r - L_h^2)}(\psi_{sb}\cdot\psi_{ra} - \psi_{sa}\cdot\psi_{rb}) \quad (2)$$

Similarly to [1], we determine the sector of the flux by comparing its components ψ_{sa}, ψ_{sb} with three digital comparators (α_0, α_{60}, α_{120} in fig. 3, calculated in fig. 1 ③). The actual torque, given by eq. (2), is compared with its reference value. The outputs of the comparators and the result of the flux controller presented below allow the choice the voltage vectors of the converter. These are classified by flux and torque increasing and decreasing vectors, as is illustrated in fig. 3. In every cycle the voltage vector is applied first, then a zero vector is switched. If the on-time of a vector is exceptionally too short, the other one is applied all over the cycle.

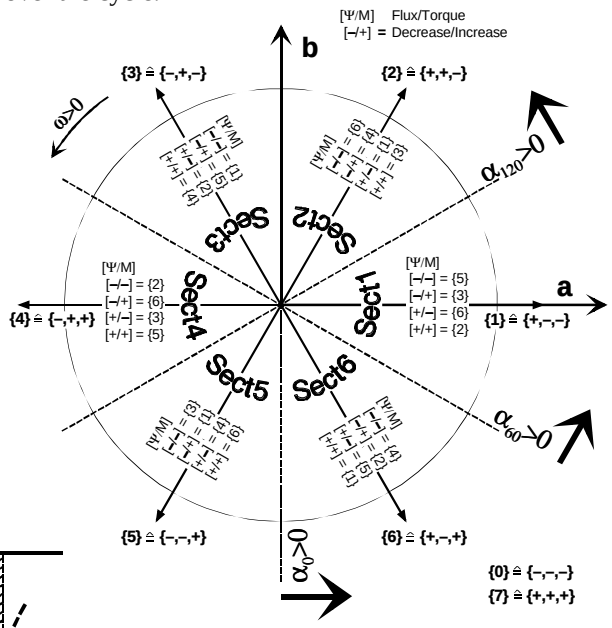

Figure 3: Voltage and Zero Vectors, Sectors

To minimize switching losses, the zero vector may be chosen in a way that at most one phase has to be switched as shown in table 1.

TABLE 1 - Selection of voltage vectors (VV)

{voltage/zero vector}	0	1	2	3	4	5	6	7
{succeeding zero vect.}	0	0	7	0	7	0	7	7

This choice of the ZV has the inconvenience that the maximum switching frequency of a switching device can be exceeded at low speed. In this case, the flux vector stays over a long time in the same sector. Applying always the same VV and ZV over the sector, the switching frequency in the according phase may be exceeded. In this case it is preferable to alternate over succeeding cycles between the two different ZVs. I. e., this may lead to a sequence like {1}-{0}-{1}-{7}-{1}-{0}, etc. Surpassing a certain speed, the ZV is chosen according to table 1.

Proceeding from fig. 2, we define:

$$\overline{M}_{VV} = \frac{1}{2}(M(t_n) + M(t_n + \Delta t_{VV})) \quad (3)$$

$$\overline{M}_{ZV} = \frac{1}{2}(M(t_n + \Delta t_{VV}) + M(t_n + \Delta t_{cycle})) \quad (4)$$

The mean value of the torque $\overline{M}_{cycle}$ over Δt_{cycle} can be written as:

$$\overline{M}_{cycle} = (\overline{M}_{VV}\cdot\Delta t_{VV} + \overline{M}_{ZV}\cdot\Delta t_{ZV}) / \Delta t_{cycle} \quad (5)$$

[1] In this paper, torque is denoted by the character "M".

The values of $\overline{M}_{VV}$ and $\overline{M}_{ZV}$ can be approximated using the linear prediction of $M(t_n + \Delta t_{VV})$:

$$M(t_n + \Delta t_{VV}) = M(t_n) + \frac{dM_{VV}(t_n)}{dt} \cdot \Delta t_{VV} \qquad (6)$$

and $M(t_n + \Delta t_{cycle})$:

$$M(t_n + \Delta t_{cycle}) = \qquad (7)$$
$$M(t_n) + \frac{dM_{VV}(t_n)}{dt} \cdot \Delta t_{VV} + \frac{dM_{ZV}(t_n + \Delta t_{VV})}{dt} \cdot \Delta t_{ZV}$$

where (from fig. 2):

$$\Delta t_{ZV} = \Delta t_{cycle} - \Delta t_{VV} \qquad (8)$$

The derivatives of the flux components at $t=t_n$ have already to be calculated to solve eq. (1). Thus, $dM_{VV}(t_n)/dt$ can be determined by deriving eq. (2). $dM_{ZV}(t+t_n)/dt$ can be approximated by:

$$\frac{dM_{ZV}(t_n + \Delta t_{VV})}{dt} \approx \frac{M(t_n) - M(t_{old})}{t_n - t_{old}} \qquad (9)$$

We obtain (see appendix) as a final result for the switching instant (fig. 1 ②):

$$\Delta t_{VV} = \Delta t_{cycle} - \qquad (10)$$
$$\sqrt{\Delta t_{cycle}^{\,2} - \frac{2\,(M(t_n) - M_{ref})\,\Delta t_{cycle} + \frac{M(t_n) - M(t_{old})}{t_n - t_{old}} \Delta t_{cycle}^{\,2}}{\frac{M(t_n) - M(t_{old})}{t_n - t_{old}} - \frac{dM_{VV}}{dt}}}$$

It is to be mentioned that this algorithm is best suited for lower speed, where $\Delta t_{VV} < \Delta t_{ZV}$. If $\Delta t_{VV} > \Delta t_{ZV}$, this method leads to unnecessary tall torque ripple. Hence for higher speed a modified procedure is processed. It will be presented in a subsequent paper.

Flux Control

Since high dynamic torque control is our main goal, the flux controller should not interfere with it. Similar to [1] the stator flux is kept on a circular trajectory. However, the method presented here does not use additional switching events to control the flux, but does it just by the selection of an appropriate VV at the beginning of the interval. After the determination of the sector and the imposition of the torque controller, two VVs remain (fig. 3; see [1]) to be favoured by the flux controller. Here the idea is to choose the VV that offers less flux deviation at the end of its on-time (fig. 1 ④).

Normally, the two potential VVs ($\vec{U}_{n,x}$, $\vec{U}_{n,y}$) lead to different on-times ($\Delta t_{n,x}$, $\Delta t_{n,y}$) imposed by the torque controller. So we have to estimate the flux propagation for both cases. Fig. 4 presents a geometric approach, where the circular flux trajectory is approximated by a straight line in the direction ψ_{tan}.

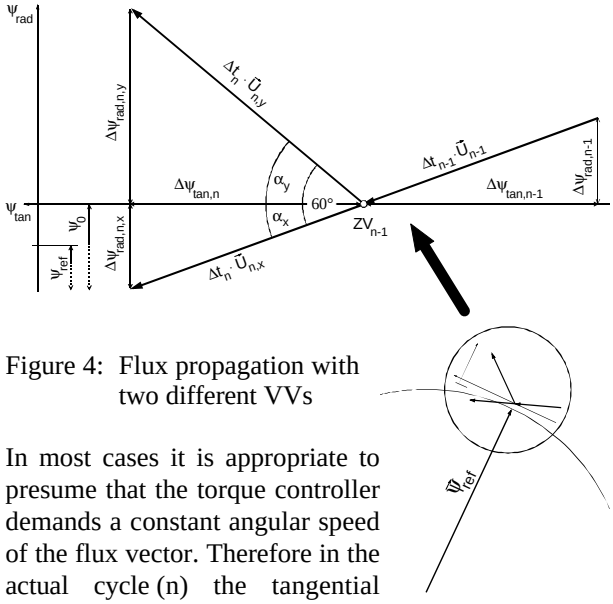

Figure 4: Flux propagation with two different VVs

In most cases it is appropriate to presume that the torque controller demands a constant angular speed of the flux vector. Therefore in the actual cycle (n) the tangential component of the flux vector will be equal to its value in the last cycle (n-1). This leads in fig. 4 to $\Delta\psi_{tan,n} = \Delta\psi_{tan,n-1}$. If the same VV as in the last cycle is chosen ($\vec{U}_{n,x} = \vec{U}_{n-1}$), the flux vector will nearly move in the same direction. Its propagation can be expressed as:

$$\Delta\psi_{rad,n,x} = \Delta\psi_{rad,n-1} \qquad (11)$$

Now we are searching for the flux propagation $\psi_{rad,n,y}$ of the alternative VV ($\vec{U}_{n,y}$) as a function of the estimated $\psi_{rad,n,x}$. It is useful to find a general expression without machine-dependent parameters. We define:

$$\Delta\psi = \Delta t_{n-1} \cdot |\vec{U}_{n-1}| = \Delta t_{n-1} \cdot \frac{2}{3} U_d \qquad (12)$$

According to fig. 4 we can define two variables x, y related to $\Delta\psi$:

$$x = \frac{\Delta\psi_{rad,n,x}}{\Delta\psi} \quad ; \quad y = \frac{\Delta\psi_{rad,n,y}}{\Delta\psi} \qquad (13)$$

As x is known from eq. 11, we are just searching for the function y=f(x). From fig. 4 we obtain:

$$\alpha_y = \frac{\pi}{3} - \alpha_x = \frac{\pi}{3} - \arcsin(x) \qquad (14)$$

$$\tan(\alpha_y) = \frac{\Delta\psi_{rad,n,y}}{\Delta\psi_{tan,n}} = \frac{y}{\frac{\Delta\psi_{tan,n}}{\Delta\psi}} \qquad (15)$$

And, with

$$\frac{\Delta\psi_{tan}}{\Delta\psi} = \cos(\alpha_x) \qquad (16)$$

this leads to:

$$y = \cos(\arcsin(x)) \cdot \tan(\frac{\pi}{3} + \arcsin(x)) \qquad (17)$$

Unfortunately, eq. (17) is rather difficult to compute in real time. A favourable approximation should be

obtained by a Taylor sequence, where the second and higher order derivatives are somewhat complicated. Analysing the error function, we have chosen as a satisfactory approximation:

$$y \approx \begin{cases} 1.538 - 2.488 \cdot x + 0.821 \cdot x^2 & \forall \; x \geq 0.5 \\ 1.733 - 3.767 \cdot x + 3.6 \cdot x^2 - 2 \cdot x^3 & \forall \; x < 0.5 \end{cases} \quad (18)$$

Using eq. 18 to determine $\Delta\psi_{rad,n,y}$, the flux controller choses

$$\vec{U}_{n,y} \text{ if } |\psi_0 + \psi_{rad,n,y} - \psi_{ref}| < |\psi_0 - \psi_{rad,n,x} - \psi_{ref}|,$$

$$\vec{U}_{n,x} \text{ otherwise.} \quad (19)$$

The equations above are valid for a $\vec{U}_{n-1}$ that decreases the flux. Similar expressions can be found for a flux increasing one (only some signs change).

Exceptional Flux Handling

Flux Decrease. If in particular operating points – mostly at low speed when the flux vector has crossed a sector boundary – the on-time of the voltage vectors is too short over several cycles. Then it is possible that the flux cannot be kept at the desired value by torque-controlling VVs only. In this case, the priority is given to the flux controller and a mainly flux increasing vector has to be applied:

TABLE 2 - Mainly flux increasing vectors

Sector	1	2	3	4	5	6
Voltage Vector	{1}	{2}	{3}	{4}	{5}	{6}

Since these vectors appear for the torque controller as disturbances, their on-time should be as short as possible. The minimal on-time $\Delta t_{flux,min}$ for the VV results from the fact that such a VV has to compensate at least the voltage drop across the stator resistance. It can be expressed as:

$$U_{Rs} = R_s \cdot I_s = R_s \cdot \frac{\psi_s}{L_s} \quad (20)$$

At the sector boundary the radial component of the VV is given by:

$$U_{rad} = \frac{2}{3} U_d \cdot \cos(30°) \quad (21)$$

The average voltage time area deducted by U_{Rs} over the whole cycle has to be equal to the voltage time area given by the radial component of the VV applied over $\Delta t_{flux,min}$. Hence it follows:

$$U_{Rs} \cdot \Delta t_{cycle} = U_{rad,min} \cdot \Delta t_{flux,min} \quad (22)$$

Replacing U_{Rs} (eq. 20) and U_{rad} (eq. 21) in eq. 22, we obtain:

$$\frac{\Delta t_{flux,min}}{\Delta t_{cycle}} = \frac{R_s \cdot \psi_s}{\frac{2}{3} U_d \cdot \cos(30°) \cdot L_s}, \quad (23)$$

In order to return the priority in the next cycle to the torque controller, the time $\Delta t_{flux,applied}$ when the mainly flux increasing vector is applied has to be prolonged. We introduce an additional rating factor k_ψ:

$$\Delta t_{flux,applied} = k_\psi \cdot \Delta t_{flux,min} \quad (24)$$

Simulations and experiments have shown that k_ψ=1.5 satisfies the needs.

Particular Switching Order. In some special cases, after applying a mainly flux increasing VV or after a ZV all over Δt_{cycle}, $\Delta\psi_{rad,n-1}$ in eq. 11 is unknown. Thus, it is not possible to use the approximation given by eq. (17). In these cases a simple two level flux controller is practised. In the first cycle after passing a sector boundary, a regular flux increasing VV is applied.

DYNAMICAL PERFORMANCE

Due to the control strategy, for small variations, the reference value is attained in less than one cycle time. The computation time up to the moment where the VV is switched is taken into account by delaying the output signal for 40µs. Thus, the dynamic behaviour may be expected just to be a delay. To get a first approach to the Bode diagram, we simulated the system with a random reference signal inferior to 3% (=1 Nm) of the nominal torque (M_N = 33 Nm). The cycle time was of 150µs. The transfer function is given by the relation of the crosscorrelation function P_{UY} to the autocorrelation function P_{UU}. Filtering the correlation functions to get a smoother plot with fewer outliers, we obtain the plots presented in fig. 5. Without surpassing any voltage or current limit, the gain is close to 1 up to 3.5 kHz. The phase angle falls short of –180° at the same frequency. Both values seem to be excellent.

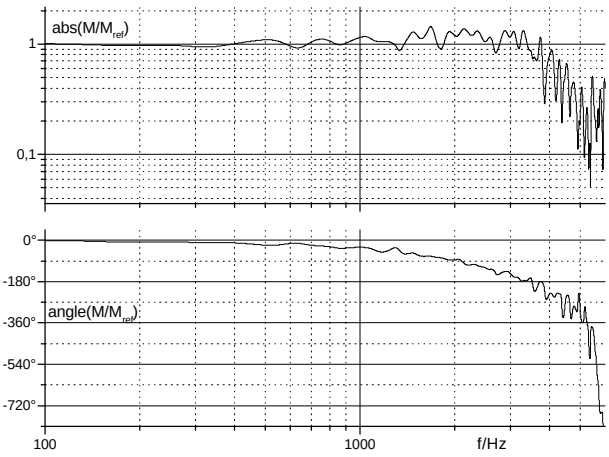

Fig 5: Bode diagram M/M_{ref} for small-signal reference (at n = 240 min^{-1} ⇔ ω = 0.16 p. u.)

For higher reference variations, a binary random reference signal of +/– 20 Nm was applied, leading to fig. 6.

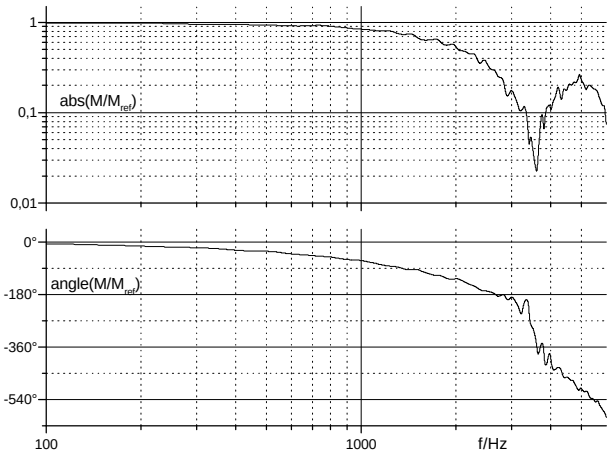

Fig. 6: Bode diagram M/M_{ref} for large-signal reference (at n = 240 min-1 $\Leftrightarrow$ ω = 0.16 p. u.)

In this case, the cut-off frequency of about 1 kHz is mainly limited by the voltage of the intermediate circuit and the stray reactance of the machine. The phase angle is above –180° even at 2.4 kHz.

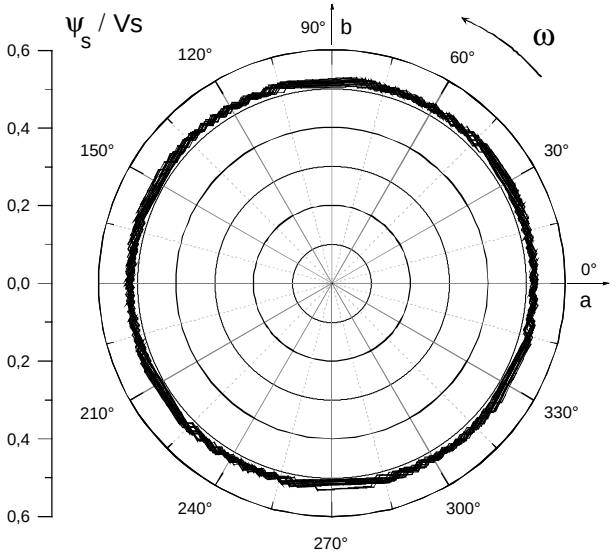

Figure 7: Typical flux trajectory

Fig. 7 shows a typical flux trajectory. Slight variations of a "virtual hysteresis width" may be recognised from the middle of a sector to its boundary.

EXPERIMENTAL RESULTS

The control scheme has been implemented on a system based on the signal processor TMS320C30 at 40 MHz. The cycle time was set to 150µs, leading to a switching frequency of 3.33 kHz per transistor. This time includes some reserves for later extensions and experimental purposes. This time may be decreased significantly as the computation time required for the DMTC algorithm is about 100µs.

Fig. 8 shows the start-up of the motor at constant setpoint of the torque of 10 Nm. At low speed the effect of flux increasing vectors can be noticed in the torque ripple. The width of the torque ripple may amaze. It has a maximum at ω = 0.5 p. u. In fact, it is due to the small leakage reactance of the machine.

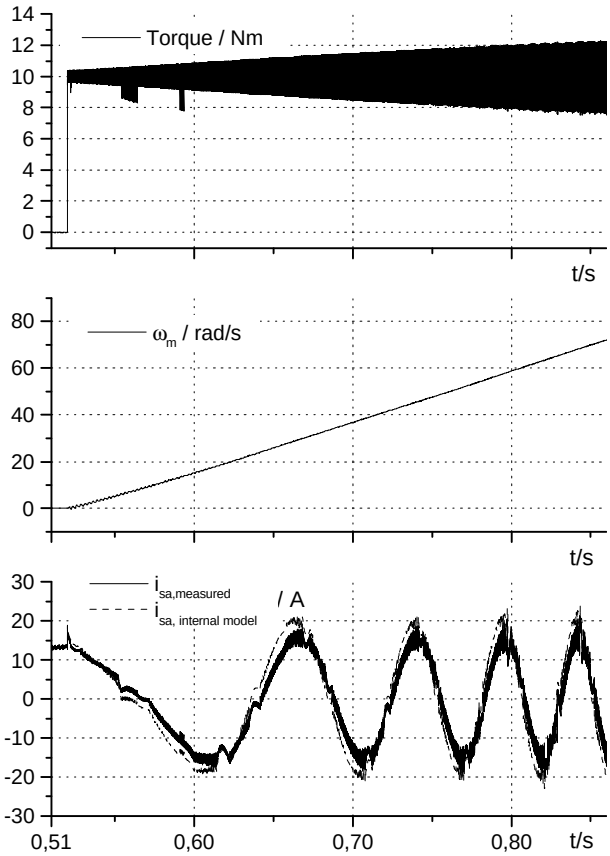

Figure 8: Start-up with constant torque reference

Fig. 9 shows the dynamic performance at a setpoint step-change of 10 Nm (ca. 30% M_N).

The delay of the measured current and the internal model is due to an additional filter on the A/D-board.

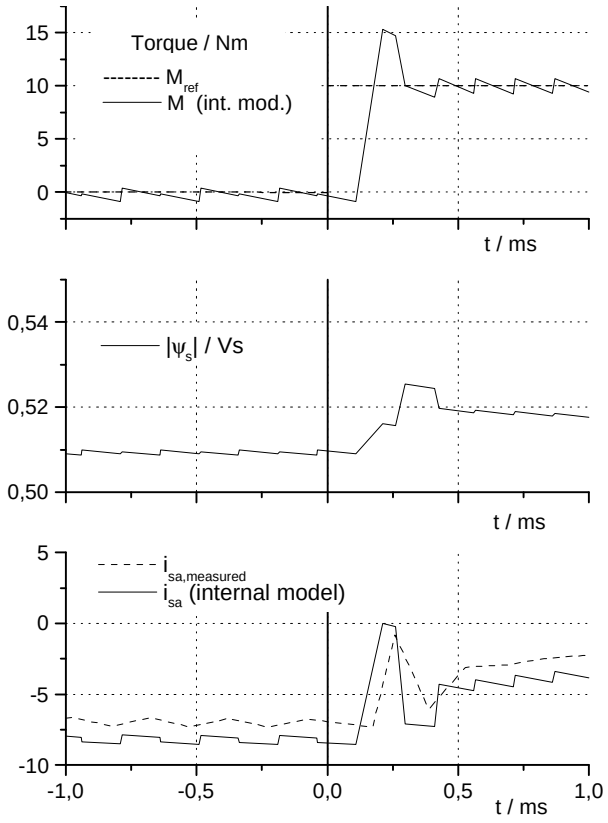

Figure 9: Torque setpoint step-change

CONCLUSION

A novel scheme to control flux and torque of an induction motor is proposed. DMTC is optimised for digital implementation at constant switching frequency, offering high dynamics particularly in an entirely digital control environment with synchronised control tasks. The algorithm proposed in this paper is suitable for lower speed. A further publication may show the enlargement for higher speed.

REFERENCES

[1] Takahashi, I., and Noguchi, T.: "A New Quick-Response and High-Efficiency Control Strategy of an Induction Motor", IEEE Transactions of Industry Applications, Vol. IA-22, No. 5, Sept./Oct. 1986)

[2] Depenbrock, M.: "Direkte Selbstregelung (DSR) für hochdynamische Drehfeldantriebe mit Stromrichterspeisung", etzArchiv, Bd. 7, 1985, Heft 7, S. 211-218

PARAMETERS

R_1	=	0.79	Ω	L_1	=	66.57	mH	Z_p	=	2		f_N	=	50	Hz
R_2	=	0.76	Ω	L_2	=	66.59	mH	n_N	=	1500	min^{-1}	M_N	=	33	Nm
L_h	=	65.	mH	ψ_{ref}	=	0.52	Vs	U_d	=	540	V				

APPENDIX

Derivation of eq. 10

To obtain eq. 10, we begin with employing the equations 8 and 9 in eq. 7. We obtain:

$$M(t_n + \Delta t_{cycle}) = M(t_n) + \frac{dM_{VV}(t_n)}{dt} \cdot \Delta t_{VV} + \frac{M(t_n) - M(t_{old})}{t_n - t_{old}} \cdot (\Delta t_{cycle} - t_{VV}) \tag{25}$$

Using eq. 6 in eq. 3, we get:

$$\overline{M}_{VV} = M(t_n) + \frac{1}{2} \frac{dM_{VV}(t_n)}{dt} \cdot \Delta t_{VV} \tag{26}$$

In the same manner we employ the equations 6 and 25 in eq. 4. This leads to:

$$\overline{M}_{ZV} = M(t_n) + \frac{dM_{VV}(t_n)}{dt} \cdot \Delta t_{VV} + \frac{1}{2} \frac{M(t_n) - M(t_{old})}{t_n - t_{old}} \cdot (\Delta t_{cycle} - t_{VV}) \tag{27}$$

We substitute some terms in eq. 5 by the eq. 26, 27 and 8:

$$\overline{M}_{cycle} = \left(M(t_n) \cdot \Delta t_{cycle} + \frac{dM_{VV}(t_n)}{dt} \Delta t_{VV} \cdot (\Delta t_{cycle} - \frac{\Delta t_{VV}}{2}) + \frac{M(t_n) - M(t_{old})}{2\,(t_n - t_{old})} \cdot (\Delta t_{cycle} - \Delta t_{VV})^2 \right) \frac{1}{\Delta t_{cycle}} \tag{28}$$

Now we set $\overline{M}_{cycle} = M_{ref}$ and solve this equation to get Δt_{VV}. This leads to eq. 10.